Trans-2-nonadecyl-4-(hydroxymethyl)-1,3-dioxolane (TNHD) purified from freshwater clams markedly alleviates dimethylnitrosamine-induced hepatic fibrosis

Trans-2-nonadecyl-4-(hydroxymethyl)-1,3-dioxolane (TNHD) purified from freshwater clams markedly alleviates dimethylnitrosamine-induced hepatic fibrosis

Ya-Ru Kuo [a], Chen-Yu Tsai [c], Wei-Sheng Lin [a], Chi-I Chang [b], Ching-Shu Lai [c], Min-Hsiung Pan [a,d,e,]*

[a] Institute of Food Sciences and Technology, National Taiwan University, Taipei 10617, Taiwan
[b] Department of Biological Science and Technology, National Pingtung University of Science and Technology, Pingtung 91201, Taiwan
[c] Department of Seafood Science, National Kaohsiung University of Science and Technology, Kaohsiung 81157, Taiwan
[d] Department of Medical Research, China Medical University Hospital, China Medical University, Taichung 40402, Taiwan
[e] Department of Health and Nutrition Biotechnology, Asia University, Taichung 41354, Taiwan

Abstract

Liver fibrosis occurs due to injury or inflammation, which results in the excessive production of collagen and the formation of fibrotic scar tissue that impairs liver function. Despite the limited treatment options available, freshwater clams may hold promise in the treatment of liver fibrosis. In this study, we demonstrated the effects of ethanol extract of freshwater clam (FCE), ethyl acetate extract of FCE (EA-FCE), and trans-2-nonadecyl-4-(hydroxymethyl)-1,3-dioxolane (TNHD) on liver fibrosis induced by dimethylnitrosamine (DMN). Administration of FCE and TNHD alleviated liver injury, including tissue damage, necrosis, inflammation scores, fibrosis scores, serum enzymes, and triglyceride levels. Furthermore, we analyzed the expression of fibrosis-related proteins, such as α-smooth muscle actin (α-SMA) and transforming growth factor (TGF-β), as well as the hydroxyproline content, which decreased after treatment with FCE and TNHD. Animal experiments revealed that FCE and TNHD can reduce liver fibrosis by inhibiting cytokines that activate stellate cells and decreasing extracellular matrix (ECM) secretion. Cell experiments have shown that TNHD inhibits the MAPK/Smad signaling pathway and TGF-β1 activation, resulting in a reduction in the expression of fibrosis-related proteins. Therefore, freshwater clam extracts, particularly TNHD, may have potential therapeutic and preventive effects for the amelioration of liver fibrosis.

Keywords: DMN-induced liver injury, Freshwater clam, Hepatic stellate cells, Liver fibrosis

1. Introduction

It is estimated that 1.5 billion individuals were affected by chronic liver disease in 2017, making it a common condition [1]. The onset of this disease can be attributed to various factors, including viral infections, autoimmune disorders, alcohol abuse, exposure to toxic chemicals, smoking, an improper diet, and metabolic disorders. These factors can lead to a range of liver diseases, such as hepatitis B and C, alcoholic liver disease (ALD), nonalcoholic fatty liver disease (NAFLD), liver fibrosis, cirrhosis, and liver cancer. So far, the strategies for treating liver injuries, such as drugs, chemotherapy, and surgery may result in several side effects and poor prognosis (in particular, cirrhosis is irreversible) [2—6]. Hence, the search for a diet or food that can alleviate or prevent liver disease has gained increased attention in recent years.

The development of liver fibrosis, which is caused by prolonged liver inflammation, is considered an early indication of cirrhosis and hepatocellular carcinoma [7]. Liver cells consist of 80% parenchymal cells and 20% non-parenchymal cells. The

parenchymal cells (hepatocytes) play an important role in biochemical metabolism in the liver. Moreover, the non-parenchymal cells, including Kupffer cells, hepatic stellate cells (HSCs), natural killer (NK) cells, fenestrated endothelial cells, and cholangiocytes are fully engaged in immunity and digestion [8]. The hepatocytes, Kupffer cells, and, particularly HSCs greatly contribute to liver fibrogenesis, increasing the inflammatory response and collagen deposition in the liver. Hepatocytes activate Kupffer cells and HSCs by releasing cytokines when viruses, drugs, alcohol, and other stimuli harm the liver. Meanwhile, the inflammatory response strengthens to repair the injured liver. Reactive oxygen species (ROS) and pro-fibrogenic cytokines such as tumor necrosis factor-α (TNF-α) and TGF-β1 are further produced and secreted by Kupffer cells. TGF-β1 induces quiescent HSCs to activate and then synthesize ECM proteins. The activated HSCs transdifferentiate into myofibroblast-like cells and become enlarged, together with an increase in contractility and loss of lipid droplets. Meanwhile, the expression of cell adhesion molecules and the α-SMA protein increase [9]. The collagen type also changes to collagen type I (col1α1 and col1α2) from collagen types III and IV. Finally, the excess deposition of the ECM protein and collagen I forms fibrous scars, aggravating liver fibrogenesis [10,11].

The freshwater clam (*Corbicula fluminea*) is an edible bivalve mollusk common in Asian countries and is regarded as a bioactive seafood—especially for hepato-protection. Previous studies have shown that *C. fluminea* could alleviate alcohol-induced liver injury in mice by reducing cytochrome p4502E1 (CYP2E1) and increasing heme oxygenase-1 (HO-1) expression. Moreover, *C. fluminea* also reversed the expression levels of hepatic cytokines (IL-1β and TNF-α) and hepatic lipid metabolism (GOT, GPT, TG, and MDA) induced by alcohol [12]. In the H_2O_2-induced HepG2 cells oxidative damage test, the peptide hydrolysate isolated from *C. fluminea* exhibited outstanding antioxidant activity [13]. In CCl_4-induced liver fibrosis in mice, the water extract of *C. fluminea* deactivated the activated hepatic stellate cells (aHSCs) by suppressing cell proliferation and hepatic fibrosis-associated cytokines. The α-SMA, TGF-β, collagen I, and TNF-α expression levels in aHSCs were downregulated after treatment with *C. fluminea*. Moreover, *C. fluminea* influenced ECM-related gene (*MMP-9* and *TIMP-II*) regulation to mediate the pathogenesis of liver fibrosis [14].

Currently, there are three common chemotoxins used to induce hepatic fibrosis in animal models: DMN, carbon tetrachloride (CCl_4), and thioacetamide (TAA). Among them, the DMN model exhibits the most remarkable hepatic fibrosis based on Masson's trichrome staining and hydroxyproline. Moreover, the DMN model also resulted in the highest quantification of α-SMA-positive cell levels [15,16]. However, few studies have analyzed the effects of *C. fluminea* on liver fibrosis induced by DMN. Thus, the DMN model was chosen in this study to investigate the underlying liver fibrosis—protection activities of *C. fluminea*. Here, we extracted *C. fluminea* using ethanol and ethyl acetate, purified the extracts, and evaluated their effects on DMN-induced liver fibrosis in mice. Some crucial markers in the liver are discussed, including the tissue morphology, biochemical concentrations, inflammatory scale, hepatic cytokine expression (α-SMA and TGF-β), and hydroxyproline level. Our research helps shed light on the anti-liver fibrosis mechanism of the *C. fluminea* extracts.

2. Materials and methods

2.1. Chemicals

Dimethylnitrosamine (DMN) and silymarin were purchased from Sigma Chemical Co. (St Louis, MO, USA). All other chemicals used were in the purest form available commercially.

2.2. Preparation of FCE, EA-FCE, and TNHD from freshwater clam

Freshwater clam (*C. fluminea*, FC) was obtained from LiChuan Agriculture Farm (Changhua, Taiwan). The extraction method underwent modification based on a previous study [17]. First, to prepare the ethanol extract of freshwater clam (FCE), freshwater clam tissue was cut into small pieces, homogenized in a blender, and extracted three times with ethanol. The resulting supernatant was filtered and concentrated using a rotary evaporator under vacuum and then subjected to freeze-drying. Second, to prepare the ethyl acetate-extracted FCE (EA-FCE), the freeze-dried powder was extracted with ethyl acetate (FCE: water: ethyl acetate weight ratio = 1:2:3) and then subjected to freeze-drying. Third, TNHD was isolated from the EA-FCE by silica gel column chromatography (8 × 70 cm and 3.5 × 40 cm, Merck 40−63 μm) and further purified using HPLC with a Phenomenex Luna C-18 column (5 mm, 250 mm × 10 mm). The sample extraction process is shown in Fig. S1. The fractions were screened for bioactivity using a cell

model, with those that showed high inhibition ability on HepG2 cells chosen and purified to obtain *trans*-2-nonadecyl-4-(hydroxymethyl)-1,3-dioxolane (TNHD) (Fig. S2A; Fig. S2B). The structure of TNHD was identified with NMR (Fig. S3).

2.3. Cell culture and treatment

The hepatic stellate cell line (HSC-T6), was cultured in Waymouth's medium supplemented with 10% fetal bovine serum (FBS) and 1% antibiotics (penicillin-streptomycin). The cells were seeded into 96-well plates at a density of 2×10^5 cells/mL and incubated in a humidified atmosphere containing 5% CO_2 at 37 °C overnight. The cells were treated with different concentrations of FCE, EA-FCE, or TNHD. After incubation for 24 h, the top layer of the medium was removed by centrifugation at 1250 rpm for 10 min and the residual medium was washed off with phosphate-buffered saline. MTT solution (0.2%, 100 μL) was added to each well and incubated for 3 h at 37 °C in 5% CO_2. Finally, the dye was dissolved with 150 μL of dimethyl sulfoxide (DMSO), and absorbance was measured at 570 nm.

The cells were seeded at a density of 2×10^5 cells/mL into 5 cm dishes and incubated overnight. Afterward, the medium was replaced with Waymouth medium (containing 0.5% FBS) and cultured for 24 h. Then, the cells were treated with different concentrations of FCE, EA-FCE, and TNHD, along with TGF-β1, for 1 h. Subsequently, the upper medium was removed, and the cells were washed with PBS to remove any residual medium. The cells were then incubated with Waymouth medium (containing 0.5 % FBS) for an additional 12 h. After this, the medium was collected by centrifuging at 3000 rpm for 5 min to collect the cell pellets. Finally, the cellular proteins were extracted for subsequent protein analysis.

2.4. Reactive oxygen species (ROS) assay

HSC-T6 cells were cultured at 2×10^5 cells/mL in 0.5% FBS. After being cultured for 12 h, the cells were treated either with TGB-β1 (1 ng/mL) in the presence and absence of FCE (10 μg/mL), EA-FCE (10 μg/mL), and TNHD (5, 10, and 25 μg/mL). After 1 h, the cells were rinsed with $1 \times$ PBS and subsequently incubated with dichlorodihydrofluorescein diacetate (DCFH-DA) for 30 min. The fluorescence was measured with an excitation of 488 nm and emission of 525−540 nm.

2.5. Animals

Male Sprague−Dawley rats weighing 200−250 g were obtained from the BioLASCO Experimental Animal Center (BioLASCO, Taipei, Taiwan). All procedures were conducted in accordance with the guidelines established by the Institutional Animal Care and Use Committee of the National Kaohsiung University of Science and Technology (IACUC, NKMU, 0109-AAAP-015). The rats were housed in polypropylene cages in a controlled environment with a 12-h light/dark cycle at 25 ± 1 °C and 50% relative humidity. All animals were fed a standard diet and had access to tap water *ad libitum*. After at least 1 week of acclimation, the rats were randomly assigned to seven groups (8 rats/group) for the experiments described below.

2.6. DMN-induced hepatotoxicity

Two experiments were designed to reveal the effects of FCE and TNHD. In the case of FCE experiment, a total of 56 rats were equally divided into seven groups, with 8 rats per group. Group I served as the vehicle control group and received saline (0.1 mL/100 g bw) via intraperitoneal (*i.p.*) injection, along with distillation-distilled H_2O via oral gavage. Group II represented the hepatotoxicity group and received *i.p.* injections of 10 mg/kg bw of DMN on Mondays, Wednesdays, and Fridays for four consecutive weeks, along with daily oral administration of distillation-distilled H_2O. Group III was the positive control and received *i.p.* injections of saline, while silymarin was orally administered at a dose of 100 mg/kg bw. Groups IV to VII received *i.p.* injections of 10 mg/kg bw of DMN, along with oral administrations of FCE at doses of 20, 50, 100, and 200 mg/kg bw, respectively. In the second experiment, groups IV to VI were administered TNHD at doses of 5, 10, and 25 mg/kg bw, respectively. At the end of the experiment, all rats were euthanized for tissue sampling, and blood was collected from the heart. Blood samples were centrifuged at $2000 \times g$ for 10 min at 4 °C to separate the serum. Liver and kidney tissues were excised and divided into several portions for enzyme activity and histopathological studies.

2.7. Biochemical examinations

The method utilized for measuring the concentrations of glutamic oxaloacetic transaminase (GOT) and glutamic pyruvic transaminase (GPT) was described in a previous publication [18].

Triacylglycerol levels were measured using an automated blood analyzer (Vitros 950, Ortho Clinical Diagnostics Co., Tokyo, Japan). Three measurements were taken for each parameter, and the average value was calculated from each individual sample.

2.8. Histopathological examinations

For H&E staining, we harvested liver tissue from the largest lobe (right lobe) in a 1 cm × 1 cm block and fixed it in 10% neutral formalin for at least 24 h. Then, the blocks were dehydrated with a series of ethanol solutions, and processed for embedding in paraffin. The paraffin-embedded blocks were sectioned to approximately 3—5 mm thickness, deparaffinized, and rehydrated. The sections were then stained with hematoxylin and eosin (H&E) and Masson's trichrome and examined by pathologists (Kaohsiung Medical University, Taiwan) for evaluation. To evaluate the histopathological slides was adjusted based on relevant prior research, incorporating the Knodell, Scheuer, and METAVIR scoring systems as references [19]. All slides were presented to the pathologist for scoring, and ten random fields were selected under a microscope for each rat. Each field was then scored according to the following scoring system: 0 = no collagen; 1 = presence of collagen but no septa; 2 = presence of collagen and septa but no connective tissue; 3 = presence of collagen with a few thin connective tissue septa; 4 = presence of collagen with thick connective tissue septa. The scores of the ten fields were then summed and divided by ten to obtain the average score, which represents the true representative score of the sample. This average score served as the basis for statistical analysis and comparisons.

2.9. Western blotting

Liver tissues were washed with PBS and lysed in an ice-cold lysis buffer (10% glycerol, 1% Triton X-100, 1 mM Na_3VO_4, 1 mM EGTA, 10 mM NaF, 1 mM $Na_4P_2O_7$, 20 mM Tris buffer (pH 7.9), 100 mM β-glycerophosphate, 137 mM NaCl, 5 mM EDTA, and one protease inhibitor cocktail tablet (Roche, Indianapolis, IN, USA)) on ice for 1 h, followed by centrifugation at 12,000 rpm for 30 min at 4 °C. Protein concentrations were determined by the Bio-Rad protein assay (Bio-Rad Laboratories, Hercules, CA, USA). Equal amounts of total cellular protein (50 μg) were resolved by SDS-polyacrylamide mini gels and transferred onto Immobilon polyvinylidene difluoride (PVDF) membranes (Millipore, Bedford, MA, USA) as described previously [20]. The membrane was then blocked at room temperature for 1 h with blocking solution (20 mM Tris—HCl, pH 7.4; 125 mM NaCl, 0.2% Tween-20, 1% BSA, and 0.1% sodium azide). The primary antibodies were conjugated with the proteins on the membrane overnight at 4 °C. The primary antibodies (dilution 1:1000) were obtained from Cell Signaling Technology Inc. (Beverly, MA, USA) and included p-Smad2, Smad2, p-P38, p-38 p-ERK, ERK, p-JNK, and JNK. β-actin was obtained from Sigma Chemical Co., and α-SMA was obtained from Abcam (Cambridge, MA). The membrane was then washed with 0.2% TPBS (0.2% Tween-20/PBS) and subsequently probed with anti-mouse, anti-rabbit, or anti-goat IgG antibodies conjugated to horseradish peroxidase (Transduction Laboratories, Lexington, KY, USA) and visualized using enhanced chemiluminescence (Amersham Pharmacia Biotech).

2.10. Reverse transcription—polymerase chain reaction

Total RNA was extracted from the liver samples, using TRIzol reagent according to the manufacturer's instructions. The RNA content was measured at 260 and 280 nm with a UV spectrophotometer, and the RNA was stored at −70 °C until reverse transcription—polymerase chain reaction analysis. Complementary DNA (cDNA) was synthesized from 2 μg of RNA using SuperScript II Reverse Transcriptase (Invitrogen, Renfrewshire, United Kingdom) in a final volume of 20 μL. The reverse transcription reactions were performed at 50 °C for 50 min and 70 °C for 15 min using a Gene Cycler thermal cycler (Applied Biosystems). The thermal cycle conditions were initiated at 95 °C for 1 min, followed by 30 cycles of amplification (94 °C for 30 s, 58 °C for 30 s, and 72 °C for 30 s), and a final extension at 72 °C for 3 min. The PCR products were separated on 2% agarose gel and visualized by ethidium bromide staining. Amplification of β-actin was used as a control for sample loading and integrity. Reverse transcription-PCR was performed on the cDNA, using the following forward and reverse primers: α-SMA (251 bp), forward primer 5′-CGCTGAAGTATCCGATAGAACAC -3′, reverse primer 5′-CAGTTGTACGTCCAGAGGCATA-3′; TGF-β1 (527 bp), forward primer 5′- TGACGT-CACTGGAGTTGTACGGCAG-3′, reverse primer 5′- GCTTGCGACCCACGTAGTAGACGA-3′; β-actin (200 bp), forward primer 5′-AAGA-GAGGGCATCCTCACCCT-3′, reverse primer 5′-TACATGGCTGGGGTG TTGAA-3′; Collagen 1α1 (618 bp), forward primer 5′- CAGGGTATTGCTG-GACAACGTGGTG-3′, reverse primer 5′-AGACCGTTGAGTCCGTCTTTGCCA-3′; Collagen

$1\alpha2$ (618 bp), forward primer 5′- TACATGGTGAC-CAAGGAGCTCCTG-3′, reverse primer 5′-CTCCTCATCCAGGTACGCAATGC-3′.

2.11. Hydroxyproline assay

The hepatic hydroxyproline content was measured using a previous procedure [21]. Liver tissue (0.2 g) was homogenized with 6 N HCl added to the tube and hydrolyzed at 110 °C in a dry bath for 24 h. The hydrolysates were neutralized with 6 N NaOH to pH 6−7 and filtered. A standard and 2 mL of the sample were transferred into a new tube, and 1 mL of chloramine-T solution was added to the tube. Oxidation was allowed to proceed at room temperature for 20 min after vortexing for 30 s. Finally, the test tube was placed in a 60 °C water bath for 20 min to stop the reaction. Absorbance was measured at 550 nm against a reagent blank, using a spectrophotometer [22].

2.12. Statistical analysis

The data are presented as means ± S.E. Statistical significance was determined by comparing the means, using Student's t-test. A p-value of less than 0.05 was considered statistically significant.

3. Results

3.1. Effects of freshwater clam extract on the body weight and relative organ weights of the DMN-administered mice

Changes in body weight can be a reliable indicator of exposure to danger. As shown in Fig. 1A, during the 28-day experimental period, the body weight in each group exhibited a slower rate of increase compared to the control group. Previous studies have reported similar findings [23,24]. Furthermore, the TNHD group exhibited a great ability in maintaining body weight (Fig. 1B). To account for individual differences in body weight, we measured the weights of the organs (Table 1). The DMN group had significantly ($p < 0.05$) higher kidney and spleen weights and lower liver weight compared to the control group. Furthermore, when the mice previously exposed to DMN were administered the FCE, the weights of the liver and kidney tended to improve compared to those of the DMN group. However, there was no significant difference between the DMN and TNHD groups.

3.2. Effects of freshwater clam extract supplementation on histopathological evaluation of liver fibrosis

H&E staining of liver sections was used to observe the location and severity of the liver injury. In the control group, the hepatic lobule was intact and clear, and the hepatic cords were arranged radially around the central vein in a cord-like manner, with no obvious cellular infiltration. By contrast, the DMN-stimulated group exhibited cell necrosis and mononuclear lymphocyte infiltration around the central lobules and portal veins of the liver (Fig. 2). Furthermore, the DMN-administered group exhibited a disorganized hepatocyte arrangement, steatosis, cellular inflammation, bile duct proliferation, and partial damage to the liver tissue. Nonetheless, combined with FCE supplementation slightly alleviated cell necrosis and steatosis (Table 2).

Masson's trichrome staining is commonly used to observe the distribution of collagen fibers in the liver. As shown in Fig. 3, the stained collagen fibers and cytonuclei appeared in violet and black, respectively, while the cytoplasm, muscle, and erythrocytes were stained red. In the control group, collagen fibers were distributed around the central vein and portal area. However, in the DMN-treated group, the hepatic lobule was damaged and disappeared, and thick collagen fibers emerged from the central vein and portal area, proliferating and wrapping around the hepatic lobule to generate nodules of unequal size. Treatment with FCE decreased collagen fibers around the hepatic lobule (Table 3). These findings suggest that FCE contributes to the alleviation of hepatic fibrosis.

3.3. Serum biomarker determination

As shown in Table 4, the enzyme activities of GOT and GPT were significantly increased in the DMN-administered group. Different doses of FCE decreased GOT and triglycerides ($p < 0.05$). Different doses of TNHD also decreased GOT but increased the TG levels. Although GOT and GPT are commonly used as biomarkers for liver damage, they lack specificity because they are present in different organs and tissues such as the kidney, pancreas, and muscle [25]. Clinically, some patients with liver disease, particularly cirrhosis, may exhibit normal GOT and GPT levels. Therefore, relying solely on liver enzymes as a biomarker for liver damage may be insufficient.
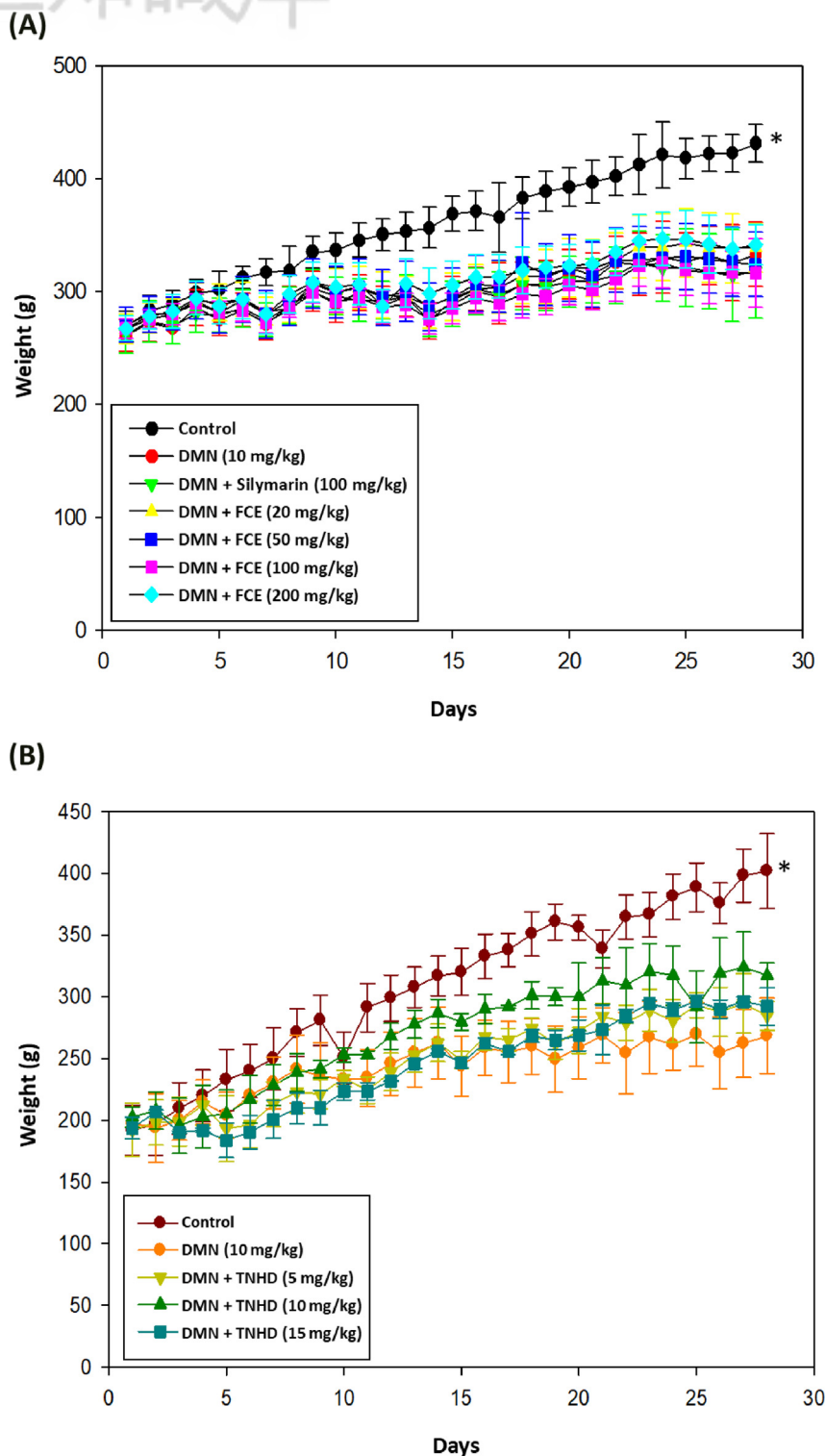
Fig. 1. Effects of FCE and TNHD on the change of body weight. DMN was administered intraperitoneally to each group, except for the control group, at a dose of 10 mg/kg for 3 days per week for 4 weeks. DMN rats were administered DMN alone; silymarin rats were administered both silymarin and DMN (A) DMN with FCE at doses of 20, 50, 100, and 200 mg/kg by oral gavage; (B) DMN with TNHD at doses of 5, 10, and 25 mg/kg by oral gavage. Data are presented as mean ± standard error (N = 8). * Indicates a significant difference from other groups (p < 0.05).

Table 1. Relative organ weight of DMN-administered rats with or without FCE and TNHD.

Groups	Relative organ weight (g/100 g of bw)		
	Liver	Kidney	Spleen
Control	3.72 ± 0.36	0.94 ± 0.09	0.21 ± 0.01
DMN	3.28 ± 0.49[#]	1.21 ± 0.15[#]	0.37 ± 0.10[#]
Silymarin	3.34 ± 0.62	1.15 ± 0.18	0.32 ± 0.11
FCE (20 mg/kg)	3.36 ± 0.21	1.09 ± 0.06*	0.39 ± 0.09
FCE (50 mg/kg)	3.34 ± 0.23	1.01 ± 0.20*	0.38 ± 0.07
FCE (100 mg/kg)	3.34 ± 0.47	1.10 ± 0.10	0.40 ± 0.10
FCE (200 mg/kg)	3.50 ± 0.37	1.16 ± 0.12	0.35 ± 0.08
Groups	Relative organ weight (g/100 g of bw)		
	Liver	Kidney	Spleen
Control	4.25 ± 0.46	0.95 ± 0.17	0.19 ± 0.00
DMN	2.17 ± 0.11[#]	0.89 ± 0.11	0.49 ± 0.11[#]
TNHD (5 mg/kg)	2.44 ± 0.03	0.61 ± 0.02	0.29 ± 0.09
TNHD (10 mg/kg)	3.13 ± 0.38	0.98 ± 0.05	0.36 ± 0.02
TNHD (25 mg/kg)	2.82 ± 0.27	0.78 ± 0.04	0.31 ± 0.00

The data represent the mean ± SD of eight rats (N = 8). DMN was intraperitoneally administered to each group except for the control group at a dose of 10 mg/kg, 3 days per week for 4 weeks. #Significantly different from the control group. *Significantly different from the DMN group, $p < 0.05$.

3.4. Effects of FCE and TNHD on protein and gene expression in the rat liver

HSCs tend to be activated from a quiescent state when the liver is injured, and α-SMA is highly expressed in activated HSCs. Stimulated and activated HSCs produce TGF-β1 and express collagen via the Smad-signaling pathway, which is then transferred to the nucleus to promote cytoskeleton reorganization and increase the expression of α-SMA [26]. Our results indicate that the α-SMA expression level in the rat liver increased after DMN induction. However, supplementation with FCE, as well as TNHD, led to a dose-dependent down-regulation of α-SMA expression. Moreover, the TNHD group showed an outstanding effect on inhibition of phospho-Smad (p-Smad) expression (Fig. 4A; Fig. 4B). In addition, we extracted the RNA in rat liver and analyzed the levels of fibrosis-related genes (*TGF-β*, *α-SMA*, *collagen 1α1*, and *collagen 1α2*) using PCR. Compared to the control group, the DMN-administered group showed an increase in *TGF-β* and *α-SMA* expression levels. However, supplementation with FCE dose-dependently decreased the expression levels of both genes, with a more pronounced effect on the *α-SMA* gene. Moreover, TNHD treatment effectively suppress the expression of DMN-induced liver fibrosis-related genes, including TGF-β, α-SMA, collagen 1α1, and collagen 1α2 gene (Fig. 5).

### 3.5. The effect of FCE on hydroxyproline concentration in DMN-induced liver injury

Liver fibrosis is strongly associated with collagen accumulation in the liver. During the process of liver tissue reconstruction and healing, abundant ECM is deposited in the wound. Collagen molecules in the connective tissue and matrix further intertwine and alter their compositions. The hydroxyproline assay is used to determine the amount of collagen present. The DMN-administered group showed the highest hydroxyproline content among all groups, indicating the most collagen accumulation. However, with FCE and, particularly, TNHD supplementation, the hydroxyproline content significantly decreased (Fig. 6). Furthermore, in TGF-β1-induced HSC-T6 cells, the expressions of p-Smad2 and α-SMA decreased after treatment with TNHD ($p < 0.05$) (Fig. 7). Based on these results, it can be demonstrated that TNHD not only exhibits a favorable effect in inhibiting DMN-induced hydroxyproline production but also demonstrates an inhibitory effect on liver fibrosis-related factors in HSC-T6 cells.

3.6. Effects of TNHD on mRNA and protein expression in TGF-β1-stimulated HSC-T6 cells

According to some studies, damaged hepatocytes and partially activated Kupffer cells and neutrophils are the main sources of ROS in the early stage of liver fibrosis. Toxic substances entering the liver are detoxified by cytochrome P450 2E1, producing free radicals that damage cells and stimulate the expression of collagen type I genes, as well as reducing the effectiveness of antioxidants. This results in excessive deposition of collagen fibers, leading to liver fibrosis [27]. We demonstrated that TNHD had a greater ROS-scavenging effect than FCE and EA-FCE in the inflammation and fibrosis
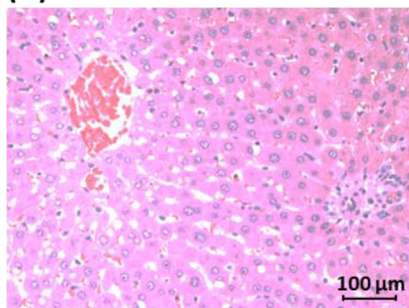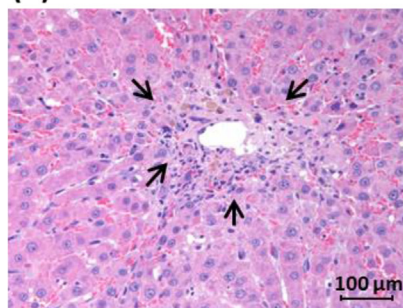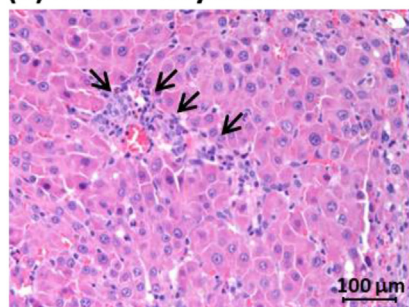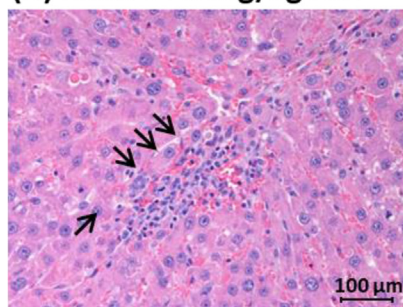
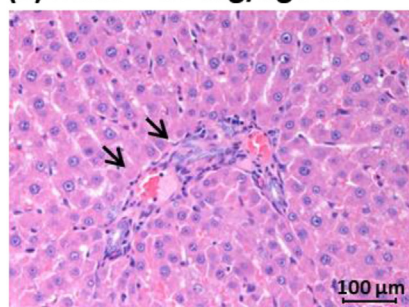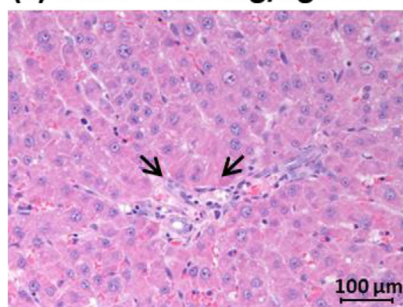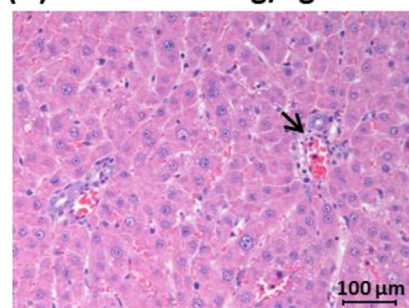*Fig. 2. **DMN-induced histopathologic changes in the liver of rats.** (A) Control group; (B) animals administered DMN (10 mg/kg); (C) animals administered both silymarin (100 mg/kg) and DMN; (D)−(G) animals administered 20, 50, 100, and 200 mg/kg FCE and DMN by oral gavage. The arrows indicate inflammatory foci (scale bar indicates 100 μm). Representative image of hepatic H&E staining (N = 8).*

responses induced by TGF-β1 within cells (Fig. S4). Moreover, we analyzed the mRNA expression of genes related to liver fibrosis, including α-SMA, TGF-β1, collagen 1α1, and collagen 1α2. From the quantitative data, it is evident that TNHD exhibits

inhibitory effects on TGF-b1, with a dose-dependent response as the dosage increases (Fig. 8). When stimulated by TGF-β1, HSC-T6 produces numerous pro-fibrotic genes. As the dose of TNHD increased, the expression of these genes decreased. TGF-β1

Table 2. Effect of FCE on fatty tissue change, bile duct proliferation, necrosis, and inflammation scores of rats in each group.

Groups	Injury of score			
	Fatty tissue change	Necrosis	Bile duct proliferation	Inflammation
Control	0.5 ± 0.6	0.0 ± 0.0	0.0 ± 0.0	0.0 ± 0.0
DMN	0.0 ± 0.0	1.0 ± 0.0[#]	2.0 ± 0.0[#]	3.0 ± 0.0[#]
Silymarin	0.5 ± 0.6	2.5 ± 0.6*	2.0 ± 0.0	2.5 ± 0.6
FCE (20 mg/kg)	0.0 ± 0.0	1.0 ± 0.0	1.5 ± 0.6	1.5 ± 0.6*
FCE (50 mg/kg)	0.0 ± 0.0	1.0 ± 0.0	1.0 ± 0.0*	2.0 ± 0.0*
FCE (100 mg/kg)	0.0 ± 0.0	1.5 ± 0.6	1.5 ± 0.6	2.0 ± 0.0*
FCE (200 mg/kg)	0.5 ± 0.6	1.0 ± 0.0	2.0 ± 0.0	2.0 ± 0.0*

Scores: 0 = no; 1 = trace; 2 = weak; 3 = moderate; 4 = strong. The data represent the mean ± SD of eight rats. DMN was administered intraperitoneally to each group except for the control group at a dose of 10 mg/kg, 3 days per week for 4 weeks. [#]Significantly different from the control group (N = 8). *Significantly different from the group administered DMN alone, $p < 0.05$.

can induce HSC-T6 to activate the p38 pathway and upregulate the expressions of extracellular signal-regulated kinase 1/2 (ERK1/2) and c-Jun N-terminal kinase 1/2 (JNK1/2) proteins [28]. Our results show that TNHD suppressed MAPK activation and p-Smad2 expression (Fig. 4B; Fig. 9A). Moreover, the results indicate that TNHD did not substantially downregulate the expression of ERK1/2 and JNK1/2. Hence, we propose that TNHD inhibits the activation of p-Smad2 by interfering with the activation of MAPKs (Fig. 9A).

3.7. TNHD inhibits the TGF-β1-induced p-Smad signaling

The results in Fig. 9A show that TNHD inhibits p38 MAPK signaling phosphorylation, which interferes with Smad phosphorylation, preventing its activation and reducing the expression of α-SMA. To confirm the involvement of TNHD in the TGF-β1-induced MAPKs signaling pathway, we blocked the TGF-β1 pathway using TNHD and p38 MAPK inhibitor and conducted an electrophoretic analysis of the extracted proteins. The results in Fig. 9B demonstrate that treatment with the p38 MAPK inhibitor (SB202190) at 2 or 10 μM inhibited the expression of α-SMA. We propose that TNHD may exert its effects by inhibiting the phosphorylation of proteins, such as p38-MAPK, induced by TGF-β1 based on these findings.

4. Discussion

DMN-induced liver fibrosis is a widely used model for the study of liver fibrosis, as it closely resembles human liver fibrosis in terms of pathological features, including inflammation, fibrosis, and cirrhosis [29,30]. DMN-induced liver fibrosis is believed to be caused by oxidative stress, inflammation, and activation of HSCs [31]. DMN is metabolized by cytochrome P450 enzymes to form

highly reactive metabolites that lead to oxidative stress and lipid peroxidation [32,33]. This oxidative stress induces hepatocellular damage and necrosis, which activates inflammatory cells and promotes the release of pro-inflammatory cytokines, chemokines, and growth factors. These factors promote the activation of HSCs and their transformation into myofibroblasts, which are responsible for the excessive deposition of ECM components such as collagen [34].

Here, we found that the freshwater clam extracts decreased the liver injury-related indicators including necrosis, inflammation, and fibrosis score. The potential effects of freshwater clam extracts on liver disease have been previously studied, and researchers found that the water extract of freshwater clam (C. fluminea) exhibited excellent ameliorative effects on inflammation and antioxidant enzyme activity in a CCl$_4$-induced acute liver injury model in rats [35]. Silymarin, a medicine that is widely used as an anti-liver fibrosis agent, also decreases inflammatory cytokines [36]. Inflammation and liver fibrosis are closely related. Chronic inflammation is a key factor in the development and progression of liver fibrosis. When the liver is exposed to chronic inflammation, the Kupffer cells release pro-inflammatory cytokines, such as TNF-α, interleukin-1 (IL-1), and interleukin-6 (IL-6). Reducing inflammation and oxidative stress is a useful approach in the prevention and treatment of liver fibrosis. Hence, we further evaluated the effects of FCE on liver inflammation and oxidative stress. Compared with the DMN group, the inflammatory score was decreased in the FCE and TNHD groups (Table 2). In addition, the same trend was observed for the fibrosis score and liver section (Fig. 3; Table 3). In terms of oxidative stress, previous research has revealed that water extract of clams exhibits free radical scavenging activity, thereby reducing cell apoptosis, and have also shown its ability to inhibit HepG2 oxidative damage caused by H$_2$O$_2$ [13].
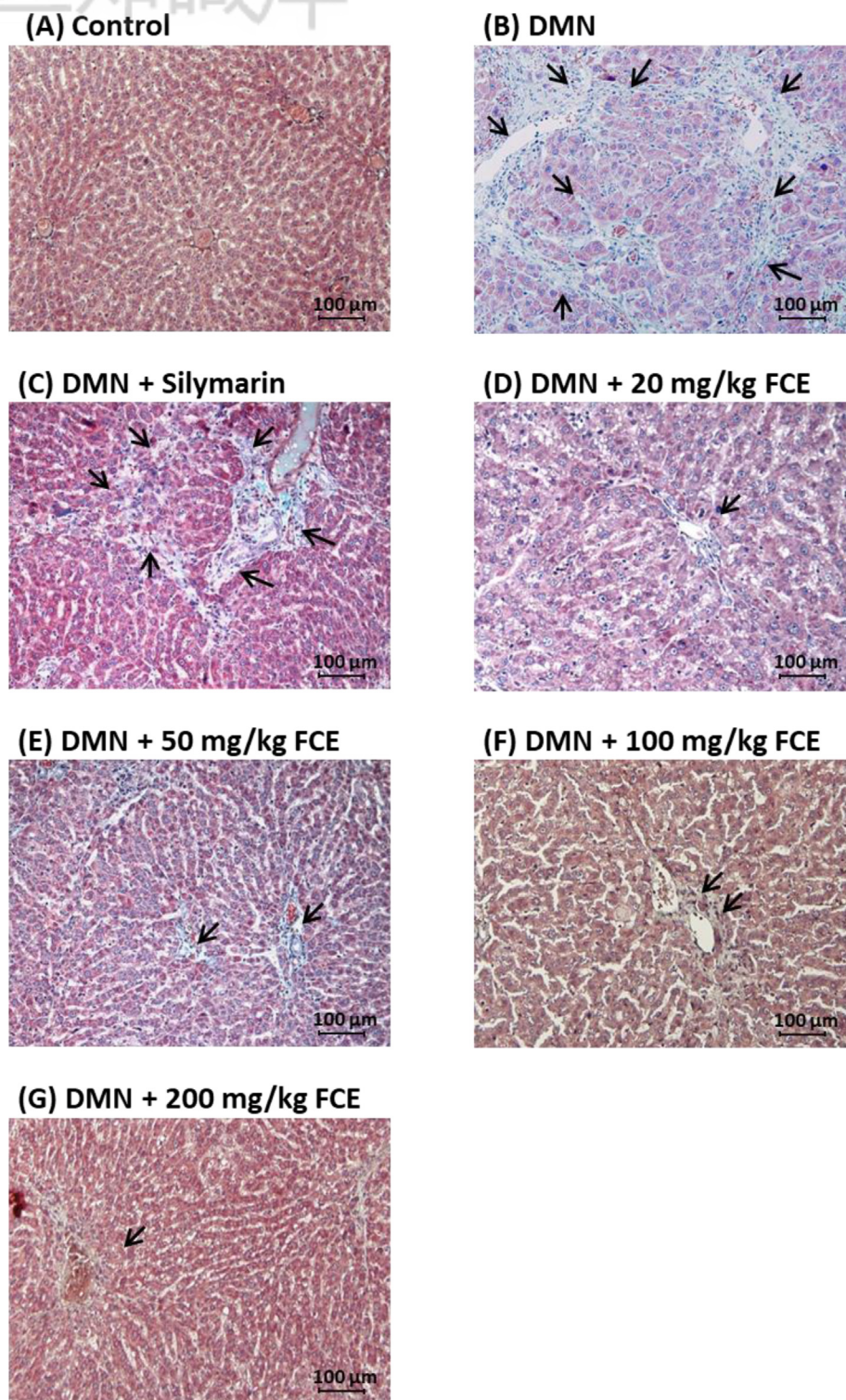
Fig. 3. *Representative photomicrograph of rat liver sections from the DMN study. Detection of collagen by Masson's trichrome staining. (A) Control group; (B) animals administered DMN (10 mg/kg); (C) animals administered both silymarin (100 mg/kg) and DMN; (D)—(G) animals administered 20, 50, 100, and 200 mg/kg FCE and DMN by oral gavage. The arrows indicate inflammatory foci. The arrows indicate the areas of DMN-induced collagen deposition (scale bar indicates 100 μm). Representative image of Masson's trichrome staining (N = 8).*

Inflammation stimulation may lead to the excessive production of ROS during oxidative metabolism. That triggers the inflammatory process and promotes the synthesis and secretion of pro-inflammatory cytokines. In the liver, external stimuli causes damage to hepatic macrophages, resulting in

Table 3. Effects of FCE on liver fibrosis scores of rats in each group.

Groups	Fibrosis scores
Control	0.0 ± 0.0
DMN	3.5 ± 0.6#
Silymarin	3.5 ± 0.6
FCE (20 mg/kg)	1.5 ± 0.6*
FCE (50 mg/kg)	1.5 ± 0.6*
FCE (100 mg/kg)	2.0 ± 0.0*
FCE (200 mg/kg)	1.5 ± 0.6*

0 = no collagen; 1 = there is collagen but no septa; 2 = there is collagen and septa but no connective tissue; 3 = there is collagen with a few thin connective tissue septa; 4 = there is collagen with thick connective tissue septa. The data represent the mean ± SD of eight rats (N = 8). #Significantly different from the control group. *Significantly different from the group administered DMN alone, $p < 0.05$.

oxidative stress and further recruit inflammatory cells. From the results of this experiment, it can be observed that FCE, EA-FCE, and TNHD effectively inhibit ROS accumulation caused by TGF-β1 (Fig. S4). Consequently, this leads to a reduction in a series of inflammatory responses, attenuating the stimulation of Kupffer cells and impacting the secretion of liver fibrosis-related factors by aHSCs. However, further evidence is required to confirm the mechanisms by which clam extracts alleviate ROS production.

Activation HSCs are critical for the progression of liver fibrosis. HSCs typically reside in the Disse space in a quiescent state, but in response to stimuli

Table 4. Effects of FCE or TNHD on serum biochemical values and lipid profiles of the rats administered DMN.

Groups	GOT (U/L)	GPT (U/L)	TG (mg/dL)
Control	108.7 ± 22.7	51.1 ± 9.3	29.1 ± 9.5
DMN	196.5 ± 56.0#	121.1 ± 39.7#	68.6 ± 17.6#
Silymarin	143.4 ± 27.6*	120.0 ± 24.5	57.0 ± 11.5
FCE (20 mg/kg)	138.7 ± 20.2*	111.0 ± 48.8	45.3 ± 6.7*
FCE (50 mg/kg)	134.4 ± 31.5*	94.3 ± 16.3	49.4 ± 10.6*
FCE (100 mg/kg)	153.3 ± 38.7	117.7 ± 35.9	46.7 ± 14.8*
FCE (200 mg/kg)	141.0 ± 16.9*	103.0 ± 17.7	49.9 ± 18.5*
Groups	GOT (U/L)	GPT (U/L)	TG (mg/dL)
Control	91.5 ± 2.12	97.5 ± 0.71	127.0 ± 8.49
DMN	168.0 ± 4.24#	201.0 ± 12.73#	67.0 ± 1.41#
TNHD (5 mg/kg)	205.0 ± 45.25	232.5 ± 71.42	89.5 ± 28.99
TNHD (10 mg/kg)	103.0 ± 20.20*	105.5 ± 0.71*	105.0 ± 6.68
TNHD (25 mg/kg)	118.5 ± 10.61*	154.5 ± 17.68*	125.0 ± 25.46

DMN was intraperitoneally administered to each group except for the control group at a dose of 10 mg/kg, 3 days per week for 4 weeks. The data represent the mean ± SD of eight rats (N = 8). #Significantly different from the control group. *Significantly different from the group administered DMN alone, $p < 0.05$.
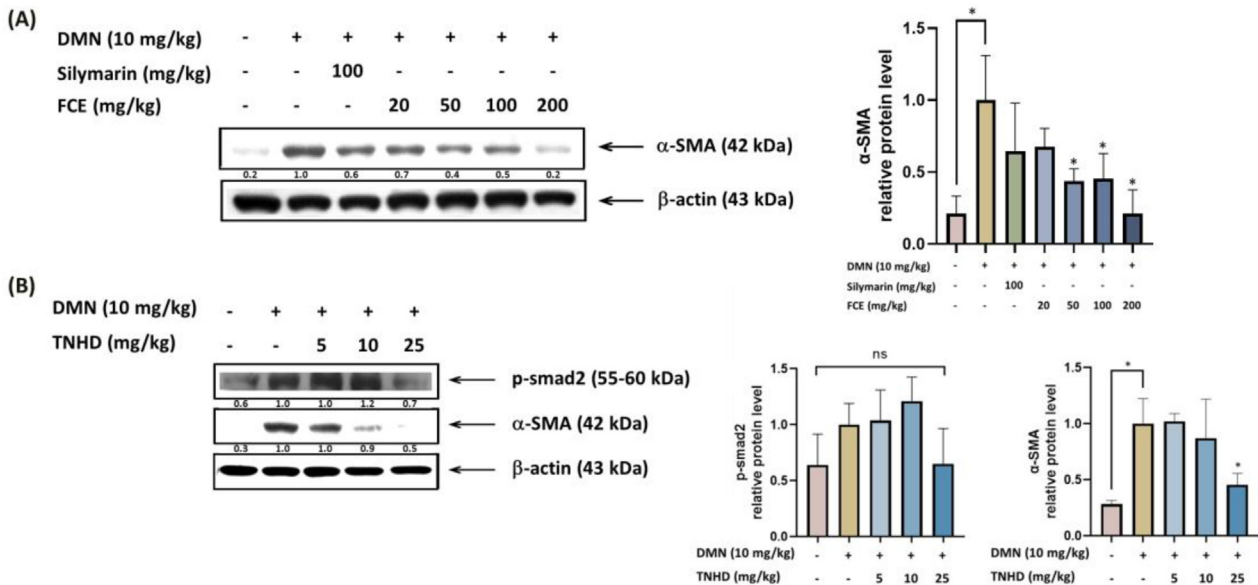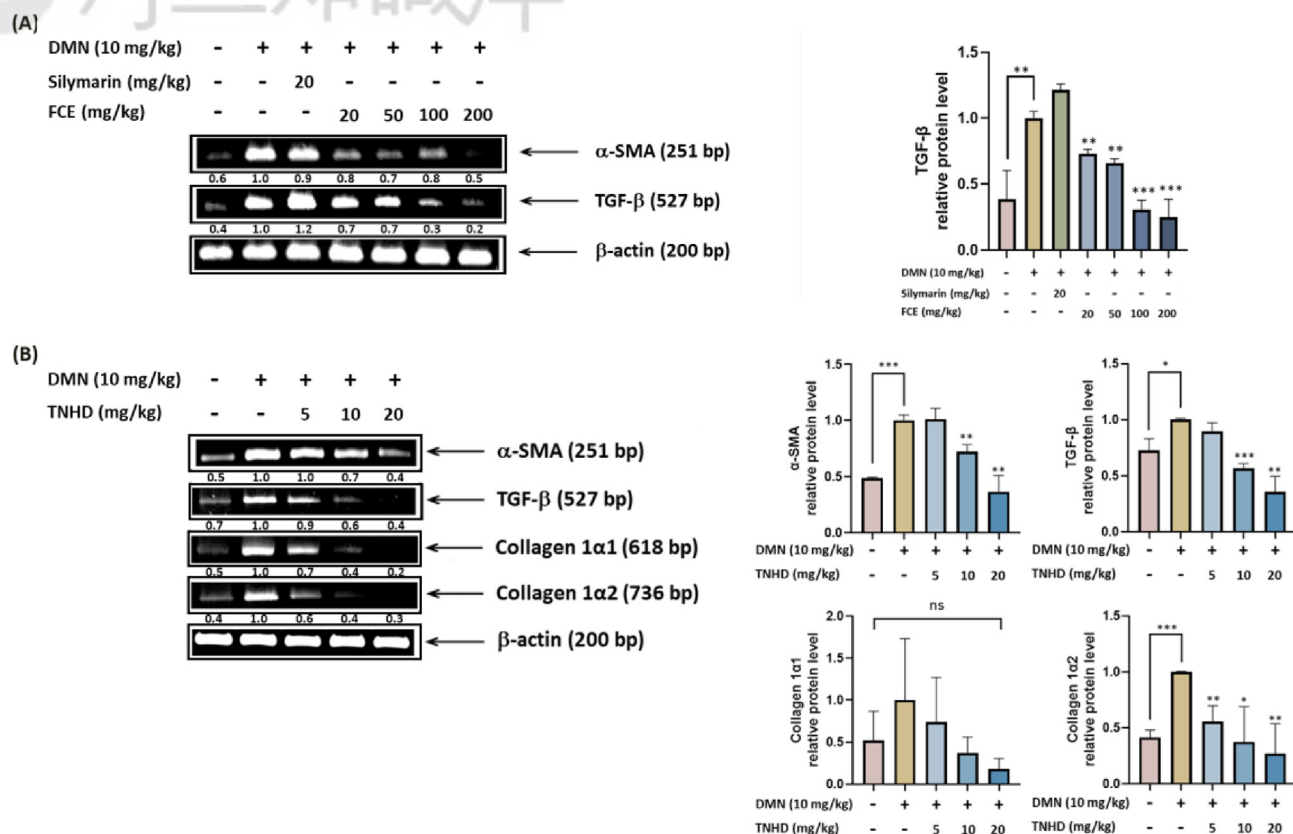

Fig. 4. Inhibitory effects of FCE and TNHD on DMN-induced protein expression in rat liver. Rats were administered 10 mg/kg of DMN alone or with different concentrations of FCE (A) and TNHD (B). The values below the figure represent the change in protein expression of the bands normalized to β-actin. All data are expressed as means ± SD. The significance of the differences was analyzed using a by two-tailed Student's t-test. Data are expressed as mean ± SD (n = 3). Different letters on data bars indicate significant differences versus the DMN group (*p < 0.05).

Fig. 5. RT-PCR analysis of the mRNA expression in the rat liver. Rats were administered 10 mg/kg of DMN alone or with different concentrations of FCE (A) and TNHD (B). Total RNA was subjected to RT-PCR with the primers α-SMA and TGF-β with β-actin as an internal control. The PCR product was resolved in 2% agarose gel. The values below the figure represent the change in protein expression of the bands normalized to β-actin. The significance of the differences was analyzed using a by two-tailed Student's t-test. Data are expressed as mean ± SD (n = 3). Different letters on data bars indicate significant differences versus the DMN group, *p < 0.05; **p < 0.01; ***p < 0.001.

and inflammation, they become activated and differentiate into myofibroblasts. Activation of Kupffer cells releases fibrogenic mediators, such as TGF-β, platelet-derived growth factor (PDGF), and connective tissue growth factor (CTGF), which stimulate HSCs to undergo activation and differentiation into myofibroblasts. These mediators induce a range of signaling pathways, including Smad, MAPK, and PI3K, leading to the upregulation of α-SMA and other myofibroblast markers [7,34,37].

The increased expression of α-SMA and other microfilaments in myofibroblasts enables them to
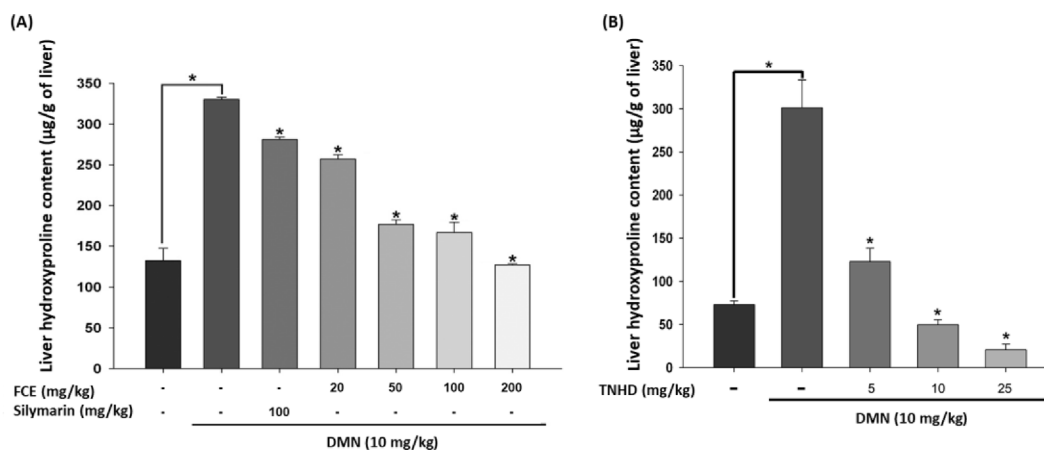

Fig. 6. Hydroxyproline content in the rat liver after 4 weeks of DMN induction (10 mg/kg) with or without different concentrations of FCE and TNHD. Data are expressed as mean ± SD (n = 3), *p < 0.005 indicate statistically significant differences from the DMN group.
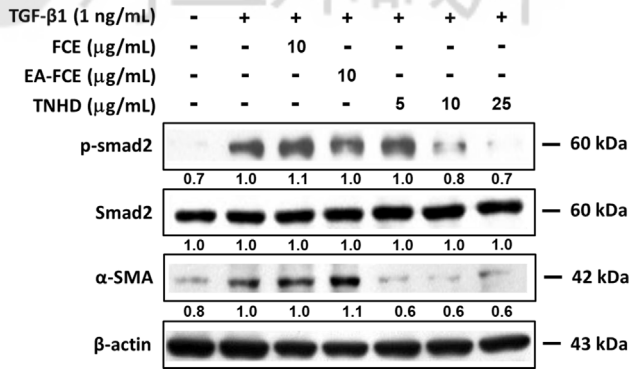
Fig. 7. Effects of FCE, EA-FCE, and TNHD on the TGF-β1-induced α-SMA, p-Smad2, and Smad2 protein expression in HSC-T6 cells. Cells were co-treated with TGF-β1 (1 ng/mL) and FCE (10 μg/mL), EA-FCE (10 μg/mL), and TNHD (5–25 μg/mL). The values below the figure represent the change in protein expression of the bands normalized to β-actin. N = 3 for Western blot analysis.

contract and produce ECM proteins, such as collagen and fibronectin. This results in the deposition of excessive ECM, leading to the development of liver fibrosis, a common consequence of chronic liver injury. Therefore, the upregulation of α-SMA and other myofibroblast markers in HSCs is a critical factor in the development of liver fibrosis [37].

Here, we confirmed that FCE, EA-FCE, and TNHD all exhibit an excellent ability to inhibit ROS generation. Moreover, after the treatment with FCE and TNHD, both the α-SMA and TGF-β protein expressions (which are highly associated with liver

fibrosis progression) were apparently decreased in the rat liver. The amount of collagen production decreased as the dosage of the extract increased ($p < 0.05$) (Fig. 4; Fig. 5). This suggests that FCE supplementation alleviates liver fibrosis by down-regulating the expression of the α-SMA protein and cytokine as well as inactivating the HSCs and Kupffer cells. Furthermore, the results of collagen staining and liver hydroxyproline content analysis show that collagen deposition in the liver was reduced after administration of the FCE supplement ($p < 0.05$) (Figs. 6–8). ECM production was lowered through the inactivation of HSCs and regulation of liver fibrosis-related gene expression. Further investigation was conducted to explore the pathways through which clam extract regulates proteins associated with liver fibrosis. One of the key factors is the cytokine TGF-β, which plays a key role in liver fibrosis. In response to liver injury or inflammation, TGF-β is released and activates the SMAD-signaling pathway, which induces the transcription of genes related to fibrosis [38–40]. Some protein expressions are investigated in a time-dependent manner. In previous studies, we observed significant differences in the expression of most proteins in the liver after treated with different samples to a 12-hr [41,42]. Therefore, we chose a single 12-hr time point and conducted the analysis under TGF-β induction to study the effect of the TNHD on protein expression. We found that TNHD may inhibit
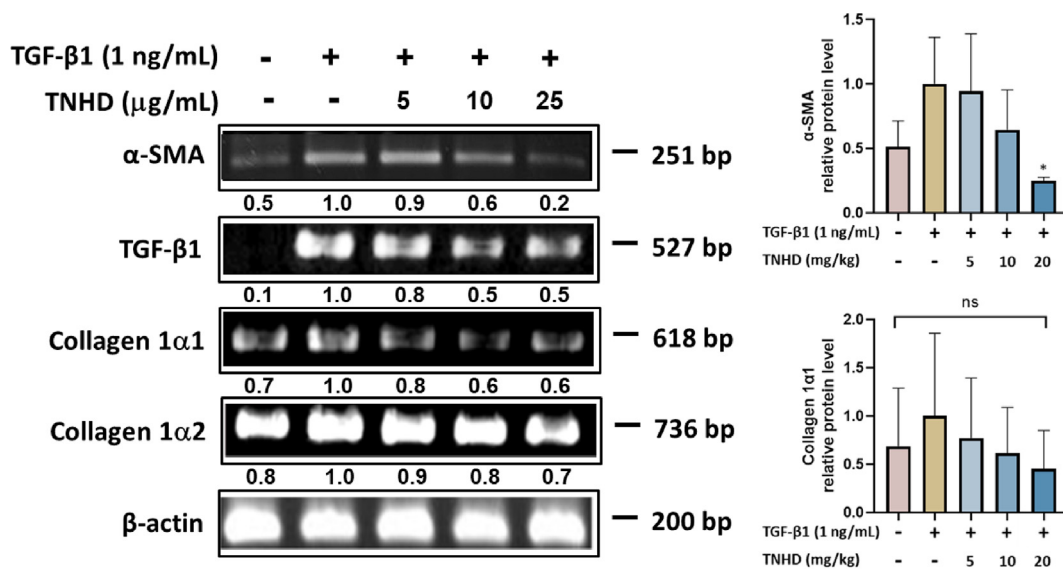

Fig. 8. RT-PCR analysis of the expression of α-SMA, TGF-β1, collagen 1α1, and collagen 1α2 mRNA. HSC-T6 cells were treated with 1 ng/mL of TGF-β1 alone or with different concentrations (5, 10, and 25 μg/mL) of TNHD for 1 h, and total RNA was subjected to RT-PCR with the primers α-SMA, TGF-β1, collagen 1α1, and collagen 1α2 with β-actin as an internal control. The PCR product was resolved in 2% agarose gel. The values below the figure represent changes in protein expression of the bands normalized to β-actin. The significance of the differences was analyzed using a by two-tailed Student's t-test. Data are expressed as mean ± SD (n = 3). Significant differences were analyzed by Student's t-test (*p < 0.05).
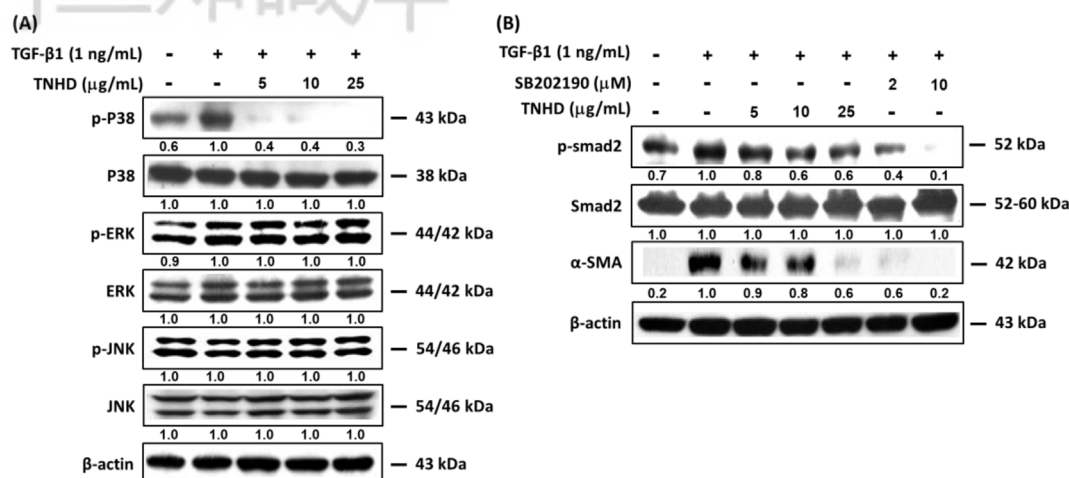
Fig. 9. Protein expression of TNHD (A) Effects of TNHD on the phosphorylation of MAPK pathways in TGF-β-induced HSC cells (B) Effects of p38 inhibitor (SB202190) and TNHD on the TGF-β-induced HSC cells. HSC cells were treated with TGF-β1 (1 ng/mL) with or without TNHD (5, 10, and 25 μg/mL) for 1 h. The liver lysates were analyzed by Western blotting. The β-actin protein level was also analyzed as a loading control. The values below the figure represent the change in protein expression of the bands normalized to β-actin. N = 3 for Western blot analysis.

fibrosis by suppressing the phosphorylation of p38 MAPK and further interfering with the phosphorylation of Smad, preventing it from entering the nucleus to become active, and reducing the expression of α-SMA, thus resulting in the inhibition of liver fibrosis (Fig. 9). Although the potential regulatory mechanism of TNHD needs further clarification, TNHD shows the potential to prevent liver fibrosis by regulating the p38 MAPK pathway.

5. Conclusion

We demonstrated the anti-fibrotic effects of the freshwater clam extracts against liver damage caused by DMN. The liver-protecting effects were evidenced by the appearance of the liver, levels of serum triglycerides and GOT, liver injury scores, the level of high fibrosis-related proteins (α-SMA and TGF-β), and the liver hydroxyproline content. The underlying effects involved anti-inflammation, inactivation of HSCs, and inhibition of both α-SMA and TGF-β production. We further demonstrated that the potential molecular mechanism of TNHD may be through the inhibition of the p38 MAPK protein phosphorylation pathway, which further affects the expression of a series of downstream liver fibrosis-related proteins. Therefore, the freshwater clam extracts have the potential to alleviate liver diseases, although further research is needed to fully understand the mechanisms of action and potential clinical applications.

Conflicts of interest

The authors declare no conflicts of interest.

Credit authorship contribution statement

Ya-Ru Kuo and **Min-Hsiung Pan**: wrote the original draft. **Chen-Yu Tsai** and **Min-Hsiung Pan**: designed the whole study. **Chi-I Chang** and **Wei-Sheng Lin** contributed to the comments and revision of the manuscript. All authors were involved in editing the manuscript.

Conflicts of interest

The authors declare no conflicts of interest.

Appendix. Supplementary data

Supplementary data provides details on the purification process of the clam extracts (FCE, EA-FCE, and TNHD) used in this study, the structure of TNHD, and some of the cell experimental results.
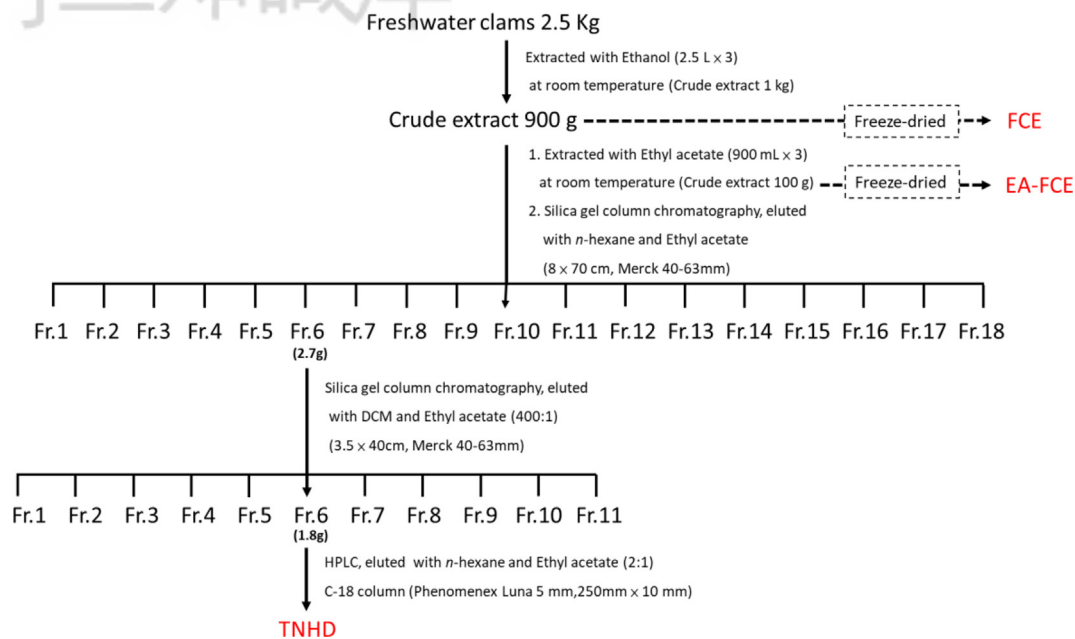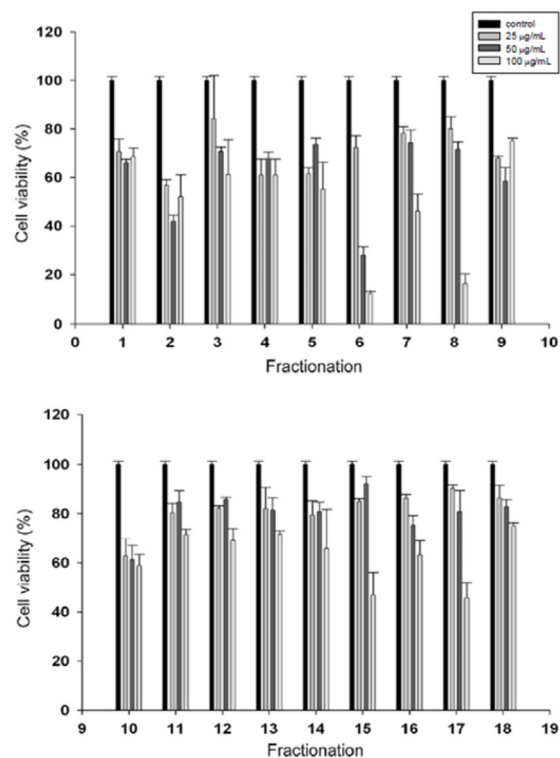
Fig. S1. Flow chart of freshwater clam extraction and purification framework.
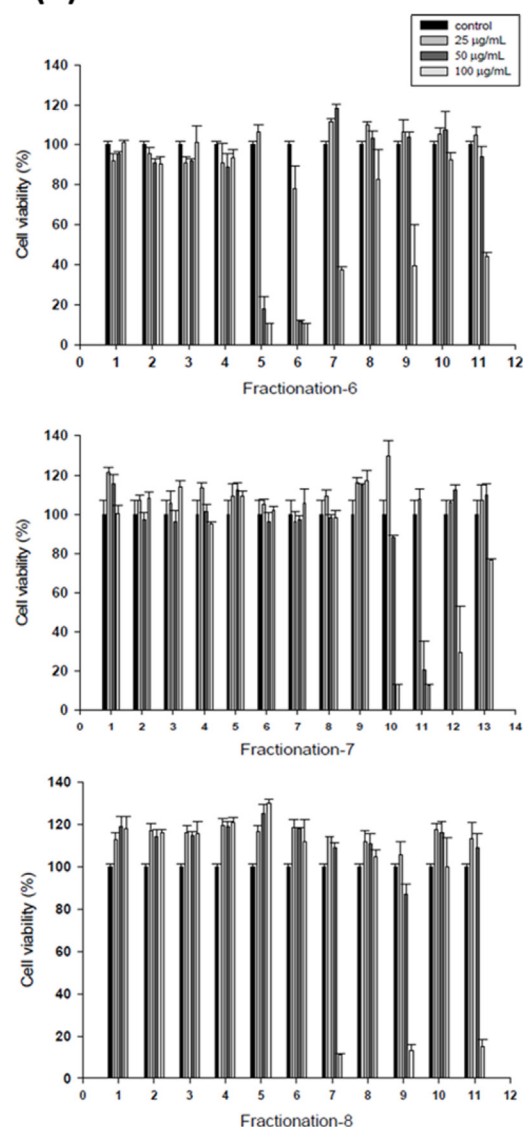
Fig. S2. *Cell viabilities of purified fractions were determined at each step of the process using Hep G2 cells. (A) The cell viability from Fr.1 to Fr.18. and (B) Fraction 6, 7 and 8 were further subjected to silica gel column chromatography (40—63 mesh) and eluted with a gradient of DCM: ethyl acetate (20:1 → 1:20). Cells were treated with various concentrations of different fraction purified from freshwater clam for 24 h. The viability of the cells was determined by MTT assay. Cells were treated with 0.1% DMSO as vehicle control. Data are expressed as mean ± SD (n = 3).*
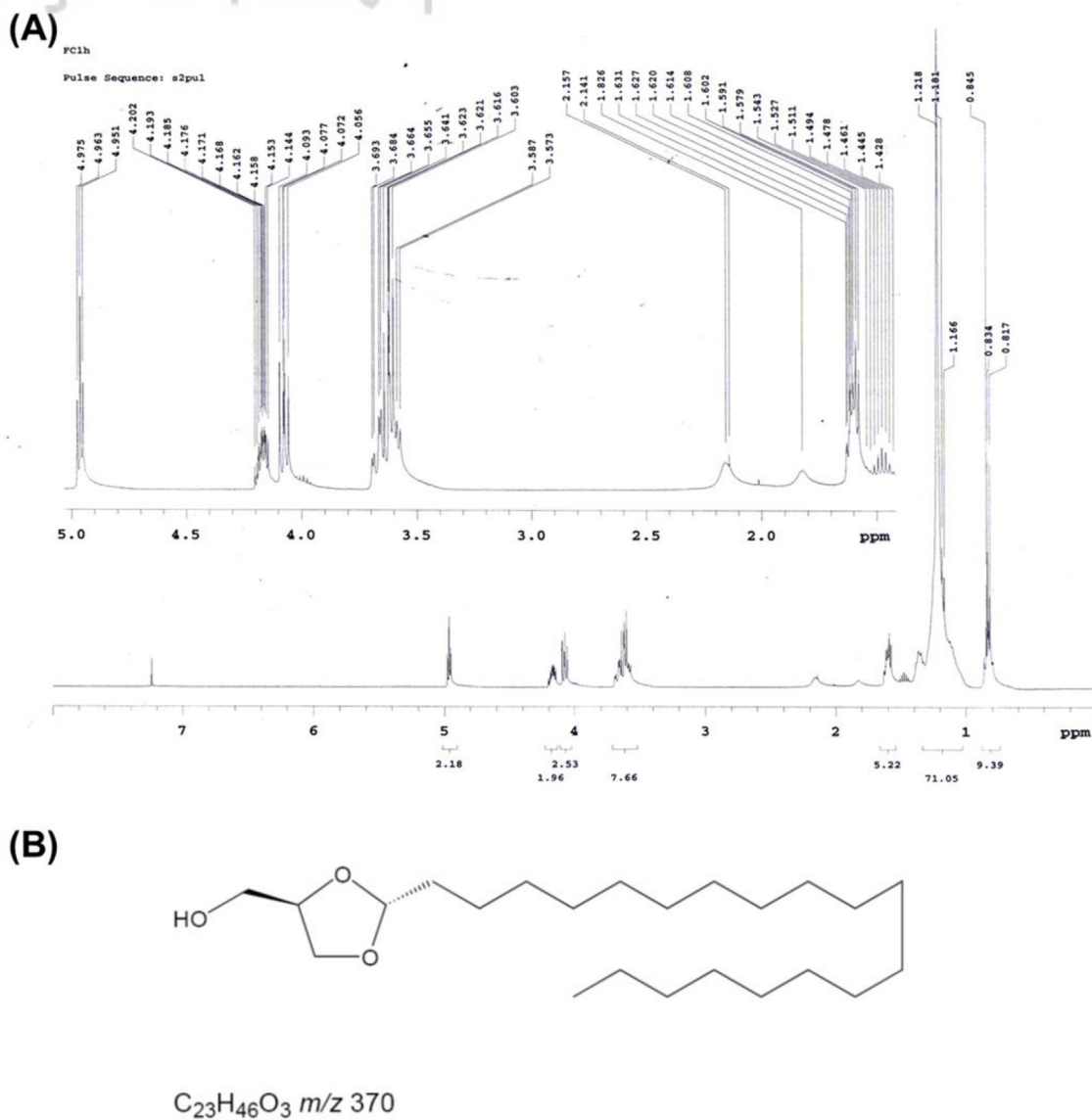
(A)

(B)

$C_{23}H_{46}O_3$ *m/z* 370

*Fig. S3. **Identification of TNHD structures by NMR.** (A) NMR spectroscopy of TNHD. (B) Chemical structure of TNHD (trans-2-nonadecyl-4-(hydroxymethyl)-1,3-dioxolane).*
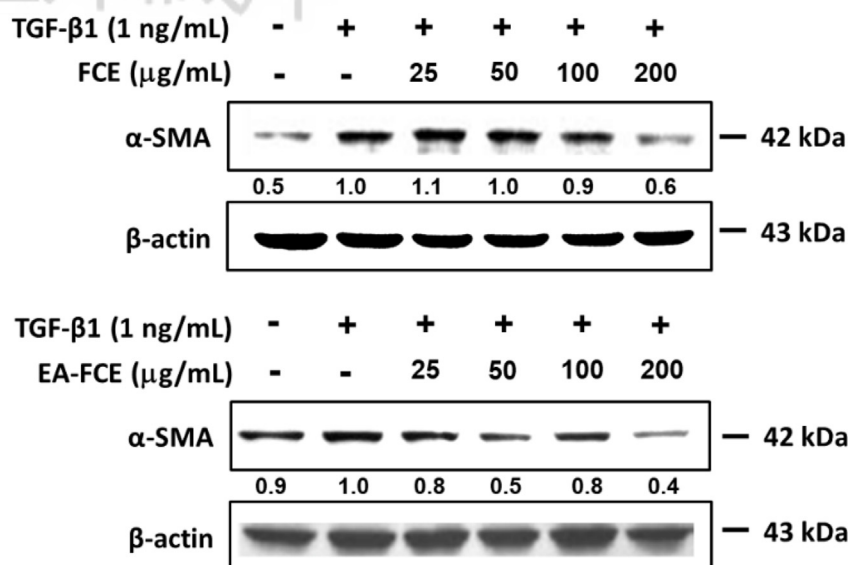
Fig. S4. Effects of FCE and EA-FCE on the TGF-β1-induced α-SMA protein expression in HSC-T6 cells. Cells were co-treated with TGF-β1 (1 ng/mL) and different concentrations of FCE and EA-FCE. After 1 h of treatment, the medium was replaced with 0.5% medium, and the cells were further incubated for 12 h. The supernatant was collected for subsequent analysis. The values below the figure represent the change in protein expression of the bands normalized to β-actin. N = 3 for western blot analysis.
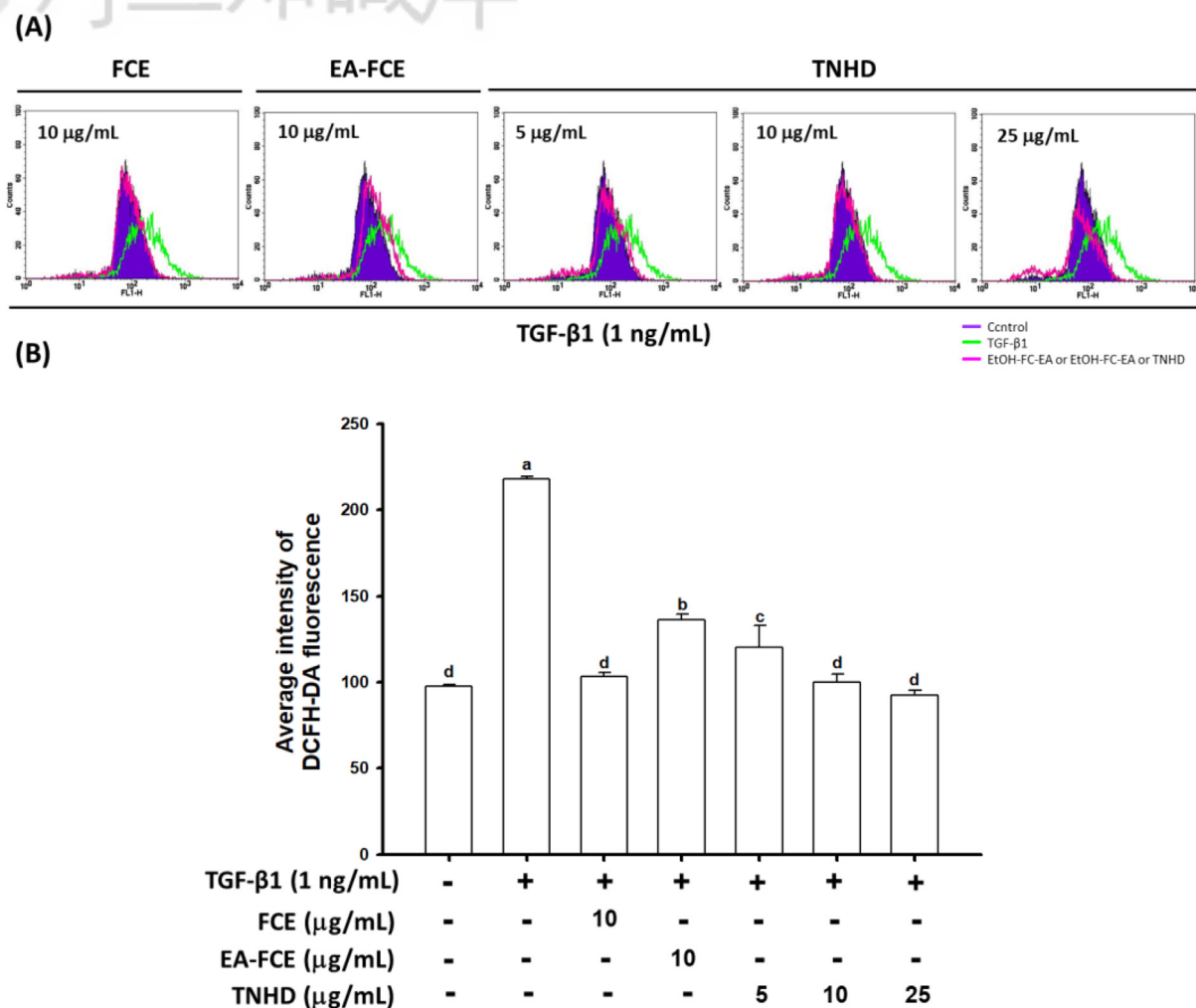
Fig. S5. Induction of peroxide in HSC-T6 cells by TGF-β1 (1 ng/mL). (A) ROS generation was measured by flow cytometry. (B) Quantification of fluorescence signals generated by reactive oxygen species (ROS). Fluorescent probe DCFH-DA was used for monitoring peroxide generation following application of 10 μg/mL FCE, EA-FCE and 5, 10, 25 μg/mL TNHD. HSC-T6 cells were treated with 10 μg/mL FCE, EA-FC, and 5, 10, 25 μg/mL TNHD for 1 h and with DCFH-DA for a further 0.5 h and the fluorescence in the cells was immediately assayed by flow cytometry. Data are presented as log fluorescence intensity. Bars labeled with different letters (a, b, c, d) on the top represent means with significantly different ($p < 0.05$) values between each group. Each bar represents the mean ± SD from at least three independent experiments and analyzed by one-way ANOVA followed by Duncan's multiple range test.

References

[1] Moon AM, Singal AG, Tapper EB. Contemporary epidemiology of chronic liver disease and cirrhosis. Clin Gastroenterol Hepatol 2020;18:2650—66.

[2] El Serag HB, Mason AC. Risk factors for the rising rates of primary liver cancer in the United States. Arch Intern Med 2000;160:3227—30.

[3] Chuang SC, Lee YCA, Hashibe M, Dai M, Zheng T, Boffetta P. Interaction between cigarette smoking and hepatitis B and C virus infection on the risk of liver cancer: a meta-analysis. Cancer Epidemiol Biomarkers Prev 2010;19: 1261—8.

[4] Borena W, Strohmaier S, Lukanova A, Bjørge T, Lindkvist B, Hallmans G, et al. Metabolic risk factors and primary liver cancer in a prospective study of 578,700 adults. Int J Cancer 2012;131:193—200.

[5] Wang P, Kang D, Cao W, Wang Y, Liu Z. Diabetes mellitus and risk of hepatocellular carcinoma: a systematic review and meta-analysis. Diabetes Metab Res Rev 2012;28:109—22.

[6] Friedman SL. Liver fibrosis—from bench to bedside. J Hepatol 2003;38:38—53.

[7] Friedman SL. Mechanisms of hepatic fibrogenesis. Gastroenterology 2008;134:1655—69.

[8] Kmieć Z. Cooperation of liver cells in health and disease. Adv Anat Embryol Cell Biol 2001;161(Iii-xiii):1—151.

[9] Gressner AM, Weiskirchen R, Breitkopf K, Dooley S. Roles of TGF-beta in hepatic fibrosis. Front Biosci 2002;7:d793—807.

[10] Kisseleva T, Brenner DA. Hepatic stellate cells and the reversal of fibrosis. J Gastroenterol Hepatol 2006;21:S84—7.

[11] Kisseleva T, Brenner D. Molecular and cellular mechanisms of liver fibrosis and its regression. Nat Rev Gastroenterol Hepatol 2021;18:151—66.

[12] Bai J, Chen Y, Ning Z, Liu S, Xu C, Yan JK. Proteoglycan isolated from Corbicula fluminea exerts hepato-protective

effects against alcohol-induced liver injury in mice. Int J Biol Macromol 2020;142:1—10.

[13] Xu H, Lv S, Jiang S, Lu J, Lin L. Radical scavenging activities of peptide from Asian clam (Corbicula fluminea) and its protective effects on oxidative damage induced by hydrogen peroxide in HepG2 cells. J Food Biochem 2020;44:e13146.

[14] Lee SL, Hsu WH, Tu CM, Wang WH, Yang CY, Lee HK, et al. The effects of freshwater clam (corbicula fluminea) extract on activated hepatic stellate cells. Evid Based Complement Alternat Med 2021:6065168.

[15] Park HJ, Kim HG, Wang JH, Choi MK, Han JM, Lee JS, et al. Comparison of TGF-β, PDGF, and CTGF in hepatic fibrosis models using DMN, CCl4, and TAA. Drug Chem Toxicol 2016;39:111—8.

[16] Yasuda M, Okabe T, Itoh J, Takekoshi S, Hasegawa H, Nagata H, et al. Differentiation of necrotic cell death with or without lysosomal activation: application of acute liver injury models induced by carbon tetrachloride (CCL4) and dimethylnitrosamine (DMN). J Histochem Cytochem 2000; 48:1331—9.

[17] Huang YT, Huang YH, Hour TC, Pan BS, Liu YC, Pan MH. Apoptosis-inducing active components from Corbicula fluminea through activation of caspase-2 and production of reactive oxygen species in human leukemia HL-60 cells. Food Chem Toxicol 2006;44:1261—72.

[18] Reitman S, Frankel S. A colorimetric method for the determination of serum glutamic oxalacetic and glutamic pyruvic transaminases. Am J Clin Pathol 1957;28:56—63.

[19] Zhou K, Lu LG. Assessment of fibrosis in chronic liver diseases. J Dig Dis 2009;10:7—14.

[20] Pan MH, Lin Shiau SY, Ho CT, Lin JH, Lin JK. Suppression of lipopolysaccharide-induced nuclear factor-κB activity by theaflavin-3,3′-digallate from black tea and other polyphenols through down-regulation of IκB kinase activity in macrophages. Biochem Pharmacol 2000;59:357—67.

[21] Jamall IS, Finelli V, Hee SQ. A simple method to determine nanogram levels of 4-hydroxyproline in biological tissues. Anal Biochem 1981;112:70—5.

[22] Lee JH, Lee H, Joung YK, Jung KH, Choi JH, Lee DH, et al. The use of low molecular weight heparin-pluronic nanogels to impede liver fibrosis by inhibition the TGF-β/Smad signaling pathway. Biomaterials 2011;32:1438—45.

[23] Lee MF, Tsai ML, Sun PP, Chien LL, Cheng AC, Ma NJ, et al. Phyto-power dietary supplement potently inhibits dimethylnitrosamine-induced liver fibrosis in rats. Food Funct 2013; 4:470—5.

[24] Chen Y, Zhou Z, Mo Q, Zhou G, Wang Y. Gallic acid attenuates dimethylnitrosamine-induced liver fibrosis by alteration of Smad phosphoisoform signaling in rats. BioMed Res Int 2018;2018:1682743.

[25] Johnston DE. Special considerations in interpreting liver function tests. Am Fam Physician 1999;59:2223.

[26] Zhu X, Kong X, Ma S, Liu R, Li X, Gao S, et al. TGFβ/Smad mediated the polyhexamethyleneguanide areosol-induced irreversible pulmonary fibrosis in subchronic inhalation exposure. Inhal Toxicol 2020;32.

[27] Kisseleva T, Brenner DA. Role of hepatic stellate cells in fibrogenesis and the reversal of fibrosis. J Gastroenterol Hepatol 2007;22(Suppl 1):S73—8.

[28] Tsukada S, Westwick JK, Ikejima K, Sato N, Rippe RA. SMAD and p38 MAPK signaling pathways independently regulate alpha 1(I) collagen gene expression in unstimulated and transforming growth factor-beta-stimulated hepatic stellate cells. J Biol Chem 2005;280:10055—64.

[29] George J, Rao KR, Stern R, Chandrakasan G. Dimethylnitrosamine-induced liver injury in rats: the early deposition of collagen. Toxicology 2001;156:129—38.

[30] George J, Chandrakasan G. Molecular characteristics of dimethylnitrosamine induced fibrotic liver collagen. Biochim Biophys Acta, Proteins Proteomics 1996;1292:215—22.

[31] Sánchez Valle V, Chávez Tapia NC, Uribe M, Méndez Sánchez N. Role of oxidative stress and molecular changes in liver fibrosis: a review. Curr Med Chem 2012;19:4850—60.

[32] Koop DR. Oxidative and reductive metabolism by cytochrome P450 2E1. Faseb J 1992;6:724—30.

[33] Godoy HM, Gomez MID, Castro JA. Mechanism of dimethylnitrosamine metabolism and activation in Rats 2. JNCI: J Natl Cancer Inst 1978;61:1285—9.

[34] Schook LB, Lockwood JF, Yang SD, Myers MJ. Dimethylnitrosamine (DMN)-induced IL-1β, TNF-α, and IL-6 inflammatory cytokine expression. Toxicol Appl Pharmacol 1992; 116:110—6.

[35] Hsu CL, Hsu CC, Yen GC. Hepatoprotection by freshwater clam extract against CCl4-induced hepatic damage in rats. Am J Chin Med 2010;38:881—94.

[36] Clichici S, Olteanu D, Nagy A-L, Oros A, Filip A, Mircea PA. Silymarin inhibits the progression of fibrosis in the early stages of liver injury in CCl4-treated rats. J Med Food 2015; 18:290—8.

[37] Gressner A, Bachem M. Molecular mechanisms of liver fibrogenesis—a homage to the role of activated fat-storing cells. Digestion 1995;56:335—46.

[38] Gauldie J, Bonniaud P, Sime P, Ask K, Kolb M. TGF-β, Smad 3 and the process of progressive fibrosis. Biochem Soc Trans 2007;35:661—4.

[39] Yang JH, Kim SC, Kim KM, Jang CH, Cho SS, Kim SJ, et al. Isorhamnetin attenuates liver fibrosis by inhibiting TGF-β/Smad signaling and relieving oxidative stress. Eur J Pharmacol 2016;783:92—102.

[40] Qin MY, Huang SQ, Zou XQ, Zhong XB, Yang YF, Zhang YT, et al. Drug-containing serum of rhubarb-astragalus capsule inhibits the epithelial-mesenchymal transformation of HK-2 by downregulating TGF-β1/p38MAPK/Smad 2/3 pathway. J Ethnopharmacol 2021;280:114414.

[41] Yu B, Jin G-n, Ma M, Liang H-F, Zhang B-x, Chen X-P, et al. Taurocholate induces connective tissue growth factor expression in hepatocytes through ERK-YAP signaling. Cell Physiol Biochem 2018;50:1711—25.

[42] Lin Y, Zhang B, Liang H-F, Lu Y, Ai X, Zhang B, et al. JNK inhibitor SP600125 enhances TGF-β-induced apoptosis of RBE human cholangiocarcinoma cells in a Smad-dependent manner. Mol Med Rep 2013;8.